Topological effects on the absorbing phase transition of the contact process in fractal media

M. A. Bab* and E. V. Albano

Instituto de Investigaciones Fisicoquímicas Teóricas y Aplicadas (INIFTA), Facultad de Ciencias Exactas, Universidad Nacional de La Plata, CCT–La Plata CONICET, Sucursal 4, CC 16, 1900 La Plata, Argentina

(Received 30 October 2008; published 24 June 2009)

In a recent paper [S. B. Lee, Physica A **387**, 1567 (2008)] the epidemic spread of the contact process (CP) in deterministic fractals, already studied by I. Jensen [J. Phys. A **24**, L1111 (1991)], has been investigated by means of computer simulations. In these previous studies, epidemics are started from randomly selected sites of the fractal, and the obtained results are averaged all together. Motivated by these early works, here we also studied the epidemic behavior of the CP in the same fractals, namely, a Sierpinski carpet and the checkerboard fractals but averaging epidemics started from the same site. These fractal media have spatial discrete scale invariance symmetry, and consequently the dynamic evolution of some physical observables may become coupled to the topology, leading to the logarithmic-oscillatory modulation of the corresponding power laws. In fact, by means of extensive simulations we shown that the topology of the substrata causes the oscillatory behavior of the epidemic observables. However, in order to observe these oscillations, which have not been reported in earlier works, the interference effect arising during the averaging of epidemics started from nonequivalent sites should be eliminated. Finally, by analyzing our data and those available on the literature for the dependence of the exponents η and δ on the dimensionality of substrata, we conjectured that for integer dimensions ($2 \leq d \leq d_c = 4$) the following exact relationship may hold: $\delta + \eta = \frac{d+2}{6}$.

DOI: 10.1103/PhysRevE.79.061123 PACS number(s): 64.60.Ht, 05.45.Df, 05.10.Ln, 05.70.Jk

I. INTRODUCTION

Continuous irreversible phase transitions (IPTs) that take place from an active state to an absorbing one share many characteristics with their reversible counterparts. One of them is the existence of a diverging correlation length when the system approaches to the critical point. Consequently, the relevant physical observables obey power laws whose exponents define the universality class of the IPT [1–3]. The contact process (CP), originally introduced by Harris [4], is a simple model that exhibits a continuous IPT for the spread of an epidemic through a network or lattice. In the network, usually taken as a hypercubic lattice, the nodes or sites can be in one of two states: "infected" (occupied, $\sigma=1$) or "susceptible" (vacant $\sigma=0$). Transitions from $\sigma=1$ to $\sigma=0$ occur spontaneously with probability λ, which is independent of the neighboring sites. On the other hand, the reverse transition, from $\sigma=0$ to $\sigma=1$, takes place with probability $1-\lambda$. In this case an occupied site autocatalytically creates a new one, in a randomly selected vacant nearest-neighbor site. Thus the state $\sigma_i=0$ for all i sites belonging to the network is absorbing and, in all dimensions, the CP undergoes a continuous (second-order) IPT into an absorbing state such that the system becomes trapped into the vacuum state. Also, λ is the control parameter governing the rate of spread of the activity, and λ_c is the critical point for the IPT. Since no exact results are available, the CP has been studied intensively via series expansion [1,5,6] and Monte Carlo simulations [1–3,6,7]. The model has attracted much interest as a prototype of a nonequilibrium critical system, and its scaling properties have been discussed extensively [1–3].

IPTs to an absorbing state have also been studied in fractal media, such as Sierpinski carpets (SCs) [8–12], percolation clusters [13,14], etc. The SC as well as other deterministic fractals are built by means of an iterative process, and then the topological details of the generating cell are present at any scale. Consequently the structure is scale invariant only for a well-defined fundamental spatial scaling ratio b, i.e., the fractal exhibits discrete scale invariance (DSI) [15]. In this way, the procedures used in order to describe some physical situations in regular lattices may not be appropriate to give a complete description of the critical behavior when the underlying media where the physical process actually takes place is a fractal. In fact, often the dynamic evolution of some observables may become somewhat coupled to a topological property of the underlying substrate leading to the occurrence of new and interesting physical situations [16].

Focusing our attention on the epidemic spread of the CP, in a recent work Lee [12] studied its critical behavior in a Sierpinski carpet, and in the checkerboard fractal, by using the epidemic analysis. In that work, dynamic observables were averaged over samples where the epidemics were initialized at randomly selected sites (RSs). In this sense, the paper of Lee [12] replicates very well-known results early published by Jensen ([9]) (see, e.g., Table I for the sake of comparison). By using this procedure the coupling between the topology of the substrate and the dynamic observables is smeared out or eventually washed out as a simple noise.

In fact, in recent papers [16,20–23] a conjecture that links the spatial DSI of fractals with the observation of time DSI in dynamic observables of physical phenomena has been proposed. Time DSI becomes evident by the occurrence of the logarithmic-periodic modulation of the power laws describing the behavior of the physical observables and is characterized by a well-defined fundamental time scaling ratio (τ). Both fundamental scaling ratios, the spatial and time ones, are linked according to $b=\tau^{1/z}$, where z is the dynamic

*mbab@inifta.unlp.edu.ar

TABLE I. Critical exponents taken from Refs. [9,12], which were obtained by averaging of the epidemics started from randomly selected sites of the SC(3,1), and the checkerboard fractals. The exponents corresponding to the universality class of directed percolation in $d=1$ and $d=2$ dimensions are also included.

Substrate	η	δ	z
SC(3,1) [12]	0.207(3)	0.443(3)	1.85(2)
SC(3,1) [9]	0.235(10)	0.40(1)	1.89(3)
Checkerboard [12]	0.282(3)	0.270(3)	1.808(3)
Checkerboard [9]	0.285(10)	0.265(5)	1.818(16)
$d=1$ [17]	0.313686(8)	0.159464(6)	1.580745(10)
$d=2$ [18]	0.2295(10)	0.4505(10)	1.76(3)
$d=2$ [19]	0.214(8)	0.460(6)	1.763(9))
$d=3$ [7]	0.114(4)	0.730(4)	1.901(5)

exponent characteristic of the physical process. Furthermore, the conjecture was tested by means of extensive computer simulations in various archetypical cases such as the dynamic behavior of the Ising magnet [16,20], the voter model as a paradigmatic example of a coarsening process without surface tension [21], the behavior of the random walk and the diffusion-controlled reaction among walkers [22,24], and the epidemic spread in several Sierpinski carpets with different fractal dimensions [23].

Within this context, the purpose of this paper is to explain why the coupling between the dynamics of the epidemic spread in the CP and the DSI of the substrate cannot be observed when the physical observables are measured by averaging epidemics started from randomly selected sites. For this purpose, we performed simulations by starting the epidemic from various (different) specific sites of the Sierpinski and the checkerboard fractals. Furthermore, we also compared the obtained results with those corresponding to epidemics averaged over randomly selected starting sites.

The paper is organized as follows: in Sec. II, we provide the definition of the contact process and give a brief description of the simulation method and the main characteristics of the fractals used. Section III is devoted to the presentation and discussion of the results. Finally, we state our conclusions in Sec. IV.

II. SIMULATION DETAILS

In order to study IPTs by means of epidemic studies, simulations are initialized by taking a configuration very close to the absorbing state. For this purpose one actually starts with the vacuum absorbing state slightly modified by adding few particles. Subsequently, the system is allowed to evolve according to the rules previously described for the CP. During this dynamic process the following quantities are recorded: (i) the average number of occupied sites $N(t)$ and (ii) the survival probability $P(t)$, which is the probability that the epidemic is still active at time t. It is worth mentioning that each single epidemic stops if the sample becomes trapped in the absorbing state, so that results have to be averaged over many different epidemics.

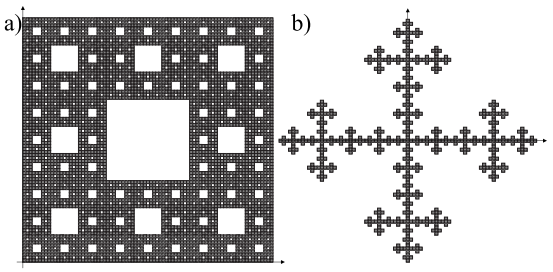

FIG. 1. (a) Sierpinski carpet SC(3,1) and (b) checkerboard fractal obtained after $k=4$ iterations. The fractal dimensions of these objects are $d_F=\log(8)/\log(3)\simeq 1.893$ and $d_F=\log(5)/\log(3)\simeq 1.465$, respectively.

By performing the epidemic at the critical point (λ_c) of a second-order IPT in fractal media, power-law behavior with log-periodic modulation due to time DSI should be assumed and the following *Ansätze* are expected to hold:

$$N(t) \propto t^{\eta} N'\left(\frac{\log t}{\log \tau}\right), \tag{1}$$

$$P(t) = t^{-\delta} P'\left(\frac{\log t}{\log \tau}\right), \tag{2}$$

where η and δ are critical exponents. Also, N' and P' are periodic functions of period one [23]. By taking advantage of this behavior one can evaluate quite accurately both the critical point and the epidemic exponents, also including the dynamic exponent z by means of the relationship $\tau=b^z$ [16,23].

In the present work we use two different types of deterministic fractals, namely a Sierpinski carpet [SC(3,1)] and the checkerboard. The generating cell of these fractals is built up by segmenting a square into 3^2 subsquares and removing one of them from the center, or the four corners, respectively (see Fig. 1). In the simulation, the segmentation process is iterated in the remaining subsquares a number k of steps. Notice that the mathematical fractal can only be obtained after an infinite number of segmentation steps, and consequently the appropriate choice of the type of boundary may be a delicate task. In our case we have used periodic boundary conditions. Since, for the case of the checkerboard fractal one has that a cell with segmentation step $k=n$ is in the center of a cell with $k=n+1$, i.e., four replicated cells become the four corners of the following generation. For the case of the Sierpinski Carpet, epidemics started from sites placed close to the center of the sample that never reach the edges are free of boundary effects. On the other hand, those epidemics started from sites placed close to the boundaries may become influences by that undesirable effect due to the fact that some fraction of the total epidemics may cross over the boundary. While along the simulations we were unable to detect artifacts due to our choice of the periodic boundary conditions, this choice may cause small discrepancies in some measured exponents as discussed below.

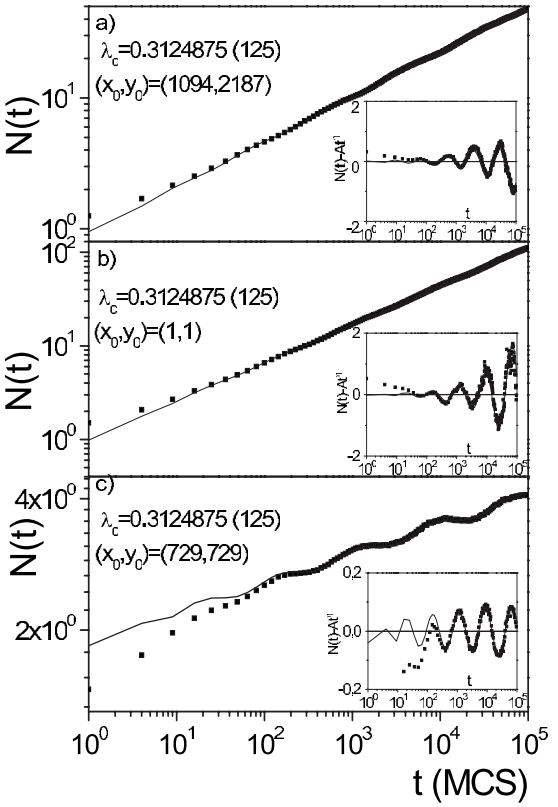

FIG. 2. Log-log plots of the number of active sites $[N(t)]$ versus time for the SC(3,1) fractal as obtained at the critical point for epidemics started at a single active site placed at the coordinates: (a) (1094,2187), (b) (1,1), and (c) (729,729). The insets show the oscillations at a linear-logarithmic scale, whose vertical axis were obtained after subtracting the modulated power-law fit from the data. Results are typically averaged over 800 000 different epidemics. More details in the text.

III. RESULTS AND DISCUSSION

Figures 2(a)–2(c) show log-log plots of the number of active sites $[N(t)]$ as a function of t, obtained for the critical value of the control parameter λ, for the case of SC(3,1) fractal with $k=7$, which corresponds to a lattice of side $L=2187$. In all cases epidemics are started by placing a single active site in an otherwise vacuum state. The data shown in panels (a), (b), and (c) correspond to epidemics started from three different sites, namely, in the middle of the upper edge (1094,2187), in the corner (1,1), and in the corner of the biggest hole (729,729) of the fractal, respectively. The epidemics performed in order to approach criticality are not shown for the sake of clarity. A careful inspection of Fig. 2 reveals the presence of soft oscillations with a logarithmic period. Within the context of the interplay between spatial and time DSI the data were fitted by means of Eq. (1), where the Fourier expansion of the periodic function was taken until the first harmonic, namely,

$$N(t) = At^{\eta}\{1 + B\cos[2\pi \log(t)/\log(\tau) + \phi]\}, \qquad (3)$$

where A and B are amplitudes, $\log(\tau)$ is the logarithmic period, and ϕ is the phase constant. After obtaining the best fits of the data (see Table II) we decoupled the oscillation just by subtracting the power law from the measured value of $N(t)$, as shown in the insets of Figs. 2(a)–2(c). By using this procedure the oscillatory behavior becomes clear beyond any doubt. It is worth mentioning that this subtracting procedure also allows us to obtain a quite accurate determination of the critical point because noticeable upward (downward) deviations of the oscillatory behavior are observed when the values of the control parameter are within the active (absorbing) phase of the system [23]. From the results of the fits shown in Table II it can be inferred that by starting the epidemics from different sites, the measured values of the critical control parameter (λ_c), the logarithmic period and consequently the dynamic exponent z are the same (within the error bars), but in contrast, the exponent η and the phase constant ϕ are different for each case. Table II also shows our results corresponding to epidemics initialized at randomly selected sites, and our determinations of the exponents are in excellent agreement (within the error bars) with those reported in the literature (see Table I). On the other hand, we also found that the time behavior of the survival probability of the epidemics shows a tiny oscillation. In order to fit the data we

TABLE II. Parameters obtained by fitting the number of active sites $N(t)$ and the survival probability $P(t)$ by Eqs. (3) and (4), respectively. The epidemics were initialized at a single active site of the SC(3,1) indicated by means of their coordinates. The dynamic exponent z was determined by using $\tau=b^z$ with $b=3$. The table also includes the results obtained by averaging epidemics started from randomly selected sites (RSs). More details in the text.

Initial site	Observable	Exponent	$\log(\tau)$	z	A	B	φ
(1094,2187)	$N(t)$	0.345(5)	0.880(8)	1.84(2)	0.94(4)	0.020(2)	5.5(3)
	$P(t)$	0.264(5)	0.88(2)	1.84(4)	0.59(5)	0.008(3)	3.8(4)
(1,1)	$N(t)$	0.406(2)	0.882(9)	1.85(2)	1.02(1)	0.019(1)	3.2(2)
	$P(t)$	0.211(8)			0.63(1)	0	
(729,729)	$N(t)$	0.068(5)	0.884(5)	1.85(1)	1.89(1)	0.022(2)	3.4(3)
	$P(t)$	0.531(8)	0.875(8)	1.83(2)	0.55(2)	0.013(1)	1.3(2)
(RS)	$N(t)$	0.200(5)			0.711(5)	0	
	$P(t)$	0.420(9)			0.597(6)	0	

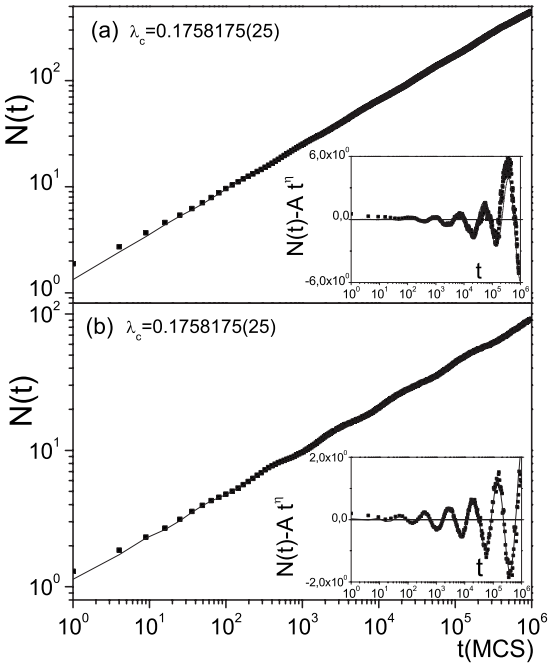

FIG. 3. Log-log plots of the number of active sites $[N(t)]$ versus time for the checkerboard fractal as obtained at the critical point for epidemics started at a single active site placed at (a) the center (0,0) and (b) the middle of the upper edge (0,3281). The insets show the shape of the oscillations in the same way as in Fig. 2. Results are typically averaged over 80 000 different epidemics. More details in the text.

used a Fourier expansion of Eq. (2) until the first harmonic, namely,

$$P(t) = At^{-\delta}\{1 + B\cos[2\pi \log(t)/\log(\tau) + \phi]\}. \quad (4)$$

However, due to the small amplitude of the oscillation for the epidemics initialized at the corner of a fractal cell, only the power-law dependence was taken into account for this case. The obtained parameters are also summarized in Table II.

The procedure already described was also used for the checkerboard fractal with lattice side $L=6561(k=8)$, as shown in Fig. 3. In this case, the epidemics are started by placing the active site in an otherwise vacuum state at (a) the center (0,0) and (b) the middle of the upper edge (0,3281) of the fractal cell. Again, Fig. 3 reveals the presence of soft oscillations that became clear after subtracting the modulated power law. Soft oscillations were also observed in the survival probability that was fitted with Eq. (4). Also, in this fractal the critical control parameter (λ_c), the logarithmic period, and the corresponding dynamic exponent z are independent of the initial site from which the epidemics begins (see Table III). For the sake of comparison, Table III also shows the results corresponding to epidemics initialized at randomly selected sites, which are in good agreement with those reported by Lee [12] and Jensen [9] (see Table I).

Summing up, the results obtained by starting the epidemics from a single site allow us to avoid the statistical interference among epidemics having different phase constants ϕ (see Tables II and III), as well as to observe the oscillations of the relevant physical observables. The excellent agreement between our estimations of the dynamic exponents and those obtained from the mean square displacement of the epidemic $[R^2(t)]$ ([9,12,23], see also Table I), strongly supports the link between the dynamics of the physical process and the topology of the underlying media where the process actually takes place.

In order to better understand the relationship between the oscillations and the fractal topology, as well as the role of the starting point, we performed a systematic study of epidemics initialized from different sites, which are equivalent after rescaling their coordinates by means of the fundamental scaling ratio. In the case of the SC(3,1), which has an infinite ramification order, one expects that the size and the distribution of holes will have a major effect on the spread dynamics. In this way, the epidemics were initialized at sites placed at the corners of the biggest hole of each generation and along the main diagonal of the fractal, i.e., the sites of coordinates $(3^n, 3^n)$, with $n=1$, 2, 3, 4, 5, and 6. The obtained results are shown in Fig. 4, and as can be observed in the main panel, for all the cases the number of the active sites shows a slow increase at the beginning of the spread, which occurs for a time that increases with the size of the nearest hole. Of course, the epidemic started at the corner of the biggest hole is the lower bound for the dynamic evolution. After this small slope regime the time behavior crosses over to that corresponding to the site nearest to the smallest hole, (1,1).

TABLE III. Parameters obtained by fitting the number of active sites $N(t)$, and survival probability $P(t)$ for epidemics initialized in a single active site placed at (a) the center (0,0) and (b) the middle of the upper edge (0,3281) of the checkerboard fractal. The dynamic exponent z was determined by using $\tau=b^z$ with $b=3$. The table also includes results obtained by a averaging epidemics starting from RSs. More details in the text.

Initial site	Observable	Exponent	$\log(\tau)$	z	A	B	ϕ
(0,0)	$N(t)$	0.422(2)	0.860(8)	1.80(2)	1.350(9)	0.013(1)	3.3(3)
	$P(t)$	0.123(1)	0.85(2)	1.78(4)	0.899(1)	0.0015(1)	1.5(1)
(0,3281)	$N(t)$	0.319(3)	0.860(4)	1.802(8)	1.108(3)	0.025(1)	0.1(7)
	$P(t)$	0.226(1)	0.861(9)	1.80(2)	0.946(2)	0.0050(1)	2.5(3)
(RS)	$N(t)$	0.282(9)			0.67(1)	0	
	$P(t)$	0.278(10)			0.75(1)	0	

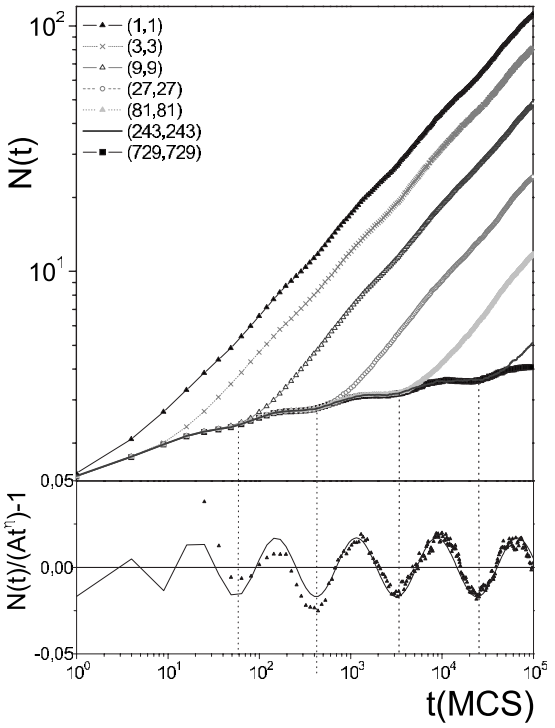

FIG. 4. Log-log plots of the time behavior, at criticality, of the number of active sites $[N(t)]$ for the SC(3,1). The epidemics were started at a single active site, whose coordinates are listed in the main panel. In order to show the relation between the oscillations and the observed crossovers in the spread of epidemics initialized from different sites, the lower panel shows the oscillation corresponding to the epidemics started at the site (1,1). More details in the text.

The lower panel of Fig. 4 shows the shape of the oscillation by the epidemics initialized at the site (1,1). From this panel the correspondence between the minimum of the oscillations and the beginning of the departure from the behavior corresponding to the epidemics initialized at the site (729,729) becomes evident. In agreement with these observations, the snapshots of the epidemics initialized at sites (81,81) and (27,27), shown in Fig. 5, indicate that for a given time, the number of active sites is larger for the epidemics started at the corner of the smallest hole. Furthermore the crossover from the small slope regime $\eta=0.068(5)$ to the large slope behavior $\eta=0.406(2)$ takes place when the epidemics reach the environment of the site (1,1).

On the other hand, the checkerboard fractal has a finite ramification order, which implies that the structure has weakly linked sites. Consequently, these sites should have the major influence on the spread of the epidemics. In order to study their effects, the epidemics were initialized at the sites $(3^{n+1},3^n)$ with $n=1,2,3,4,5$, and 6, which are self-similar by rescaling the spatial scale by the fundamental scaling ratio $b=3$. Also, the selected sites are in the center of environments that can be related to different generations. Figure 6 shows the time evolution of the number of active sites. From the main panel an initial regime is observed where the spread for all sites coincides with that corresponding to the behavior of site (0,0). After that regime, each

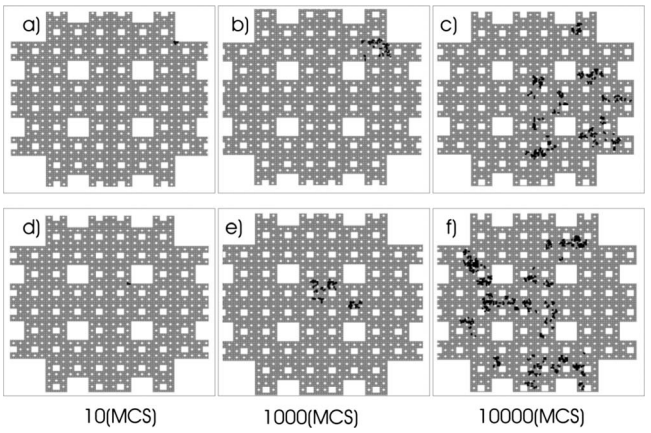

FIG. 5. Snapshots of the epidemics initialized from the sites [(a)–(c)] (81,81) and [(d)–(f)] (27,27) corresponding to relevant times determined from Fig. 4. Active sites are shown in black while fractal sites are indicated in gray. In order to consider the effects of the periodic boundary conditions the simulation cells were reassembled and the site (1,1) is in the center of the snapshot. More details in the text.

spreading exhibits a plateau whose beginning becomes shifted toward longer times when the distance from the starting site to the origin increases. From the lower panel of Fig. 6 it is inferred that the beginning of the plateau always coincides with a maximum of the oscillation corresponding to the epidemics started at site (0,0). Furthermore, after the plateau, the epidemics recover the spread behavior of the epidemics started at site (0,0). These results imply that when the spread is trapped within an environment or generation weakly linked with the fractal structure, a slowdown of the dynamics is observed. The latter assertion is supported by the

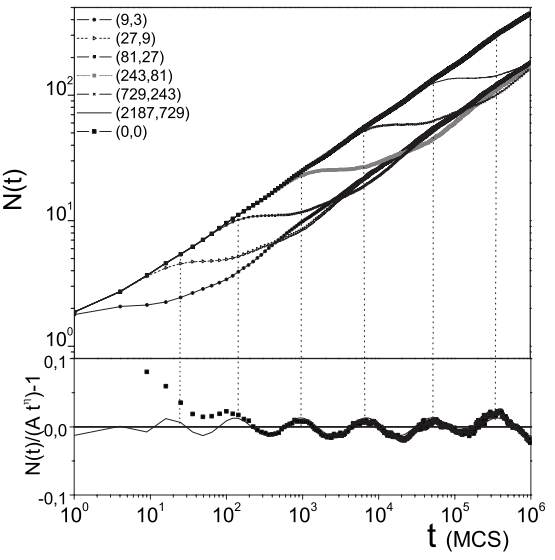

FIG. 6. Log-log plots of the number of active sites $[N(t)]$ versus time for the checkerboard fractal as obtained at the critical point. Epidemics are started at a single active site, whose coordinates are listed in the main panel. The lower panel shows the oscillation corresponding to the epidemics initialized at (0,0). More details in the text.

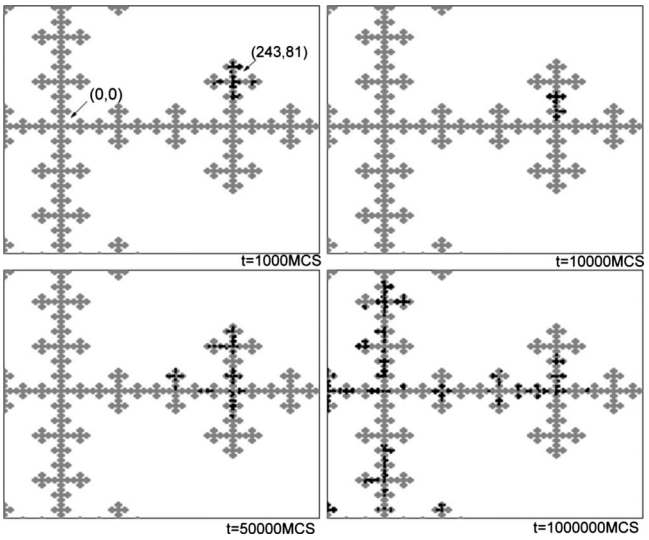

FIG. 7. Snapshots of the epidemics initialized at the site (243,81), corresponding to relevant times determined from Fig. 6. Active sites are shown in black while fractal sites are indicated in gray. More details in the text.

snapshots shown in Fig. 7, e.g., one observes a small number of active sites for $t=10^4$ MCS that corresponds to the plateau of the epidemic initialized at the same site shown in Fig. 6.

In spite of the fact that our epidemic simulations are performed during large time periods (usually involving few time decades more than in previous papers [9]), it is worth to discuss the expected long-time behavior, namely, $t\to\infty$. The fact that the amplitude of the oscillations increases (when we plot the results after subtracting the power law, as e.g., in Figs. 2 and 3) or remain constant (when we plot the results normalized by the power law, as, e.g., 4 and 6), strongly suggests that the oscillations will remain in the long-time regime. Also notice that we are able to detect up to 4–5 oscillations exhibiting the above mentioned behavior so that we can assure that for that relative long period of time the oscillation are not damped. Furthermore, for the case of random walks on fractal media, there is a number of exact analytical results showing that the oscillation remains forever [24–27]. Due to the similarity of both systems (e.g., spreading versus diffusion) we are further confident that the oscillations in the contact process will also remain for the long-time regime.

Finally, it is worth mentioning that in integer d-dimensional media, the critical exponents are not independent but they are linked according to a scaling relationship, namely, $\frac{d}{z}=\eta+\delta+\delta'$, where δ' is the exponent of the asymptotic time dependence of the density of active sites when the initial condition corresponds to a fully occupied state [28]. For the case of the studied fractals, we obtained $\delta'=0.410(9)$ (SC) and $\delta'=0.264(6)$ (checkerboard) (the results are not shown here for the sake of the space). Then, by using the obtained exponents η, δ and z (listed in Tables II and III) and δ', the scaling relationship holds if the dimension is replaced by the fractal dimension (d_F).

On the other hand, based on our observations that the dynamic exponent is independent of the starting site, one concludes that the above mentioned scaling relationship also implies that $\frac{d_F}{z}-\delta'=\eta+\delta=$const, i.e., $\eta+\delta=0.610(10)$ and $\eta+\delta=0.550(10)$ for the SC and checkerboard fractals, respectively. These figures can be compared with the results obtained in previous works (see Table I). In fact, for the SC one has $\eta+\delta=0.650(4)$ [12] and 0.635(10) [9], i.e., our results are approximately 5% off from the early work, a fact that could be due to the choice of the boundary conditions. Also, for the checkerboard fractal one has $\eta+\delta=0.552(4)$ [12] and 0.550(11) [9] in full agreement with our results. In this sense, the initial condition dependent exponents η and δ are no longer independent. In view of this finding we analyzed the available data on the dependence of spread exponents on the dimensionality, as shown in Fig. 8. While, in general, one observes a defined trend of the data for $1\leq d\leq d_c$ (d_c is the upper critical dimension for directed percolation universality class), showing that $\eta+\delta$ increases monotonically with the dimension, the linear dependence found for $d\geq 2$ is particularly striking. Since it is customary to look for rational numbers in order to obtain exact values of critical exponents, the observed behavior leads us to conjecture the following relationship:

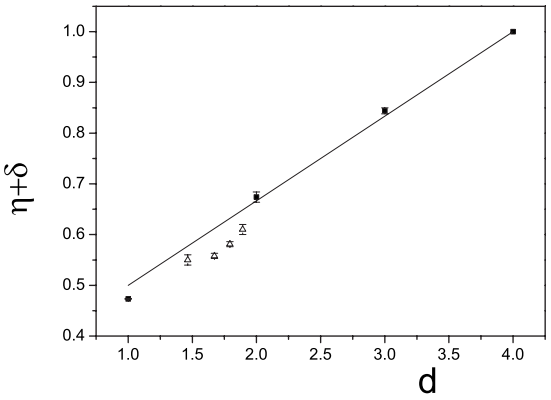

FIG. 8. Plot the exponents $\eta+\delta$ versus dimension. The data corresponding to the universality class of directed percolation (full squares) are taken from the references listed in Table I; the data corresponding to the fractals (open triangles) are taken from the present work and Ref. [23]. The solid line shows the predictions of the conjecture proposed by Eq. (5)

$$\delta+\eta=\frac{d+2}{6},2\leq d\leq d_c, \tag{5}$$

which may hold for directed percolation. In fact, Eq. (5) is consistent within the error bars, as follows: (a) for $d=2$ the prediction is $\delta+\eta=\frac{2}{3}$ and the simulations give $\delta+\eta=0.6800(14)$ [18] and $\delta+\eta=0.674(10)$ [19] (see Table I); (b) for $d=3$ the prediction is $\delta+\eta=\frac{5}{6}$ while the numerical results yield $\delta+\eta=0.844(6)$ [7]; and, of course, for $d_c=4$ Eq. (5) gives exactly the mean field value $\delta+\eta=1$.

IV. CONCLUSIONS

We studied the epidemic behavior of the contact process in a Sierpinski carpet and the checkerboard fractals, showing that time DSI becomes evident by the observation of

logarithmic-periodic modulations in the dynamic behavior of the physical observables when the epidemics are initialized at a single site. The results point out that the subtle interplay between the dynamics of the physical process and the topology of the fractal requires careful measurements in order to avoid the occurrence of interference effects that may hinder the observation of the actual physical behavior. In fact, by averaging epidemics started from randomly selected sites, the oscillations become severely damped and could be confused with simply statistical noise. In this way, by complementing the recent results of Lee [12] and early measurements of Jensen [9], we expect that the present paper will contribute to a deep understanding of the epidemic behavior of the CP in particular, and the dynamic critical behavior of directed percolation processes in general. In particular, our conjecture $\eta+\delta=$const, which is independent of the starting point of the epidemics, poses a theoretical challenge for the understanding of the widespread universality of directed percolation.

ACKNOWLEDGMENT

This work was supported financially by CONICET, UNLP, and ANPCyT (Argentina).

[1] J. Marro and R. Dickman, *Phase Transitions and Critical Phenomena* (Cambridge University Press, Cambridge, 1999).
[2] H. Hinrichsen, Adv. Phys. **49**, 815 (2000); Physica A **369**, 1 (2006).
[3] G. Ódor, Rev. Mod. Phys. **76**, 663 (2004).
[4] T. E. Harris, Ann. Probab. **2**, 969 (1974).
[5] I. Jensen and R. Dickman, Physica A **203**, 175 (1994).
[6] T. M. Liggett, *Interacting Particle Systems* (Springer, New York, 1985).
[7] I. Jensen, Phys. Rev. A **45**, R563 (1992).
[8] E. V. Albano, Phys. Rev. Lett. **69**, 656 (1992).
[9] I. Jensen, J. Phys. A **24**, L1111 (1991).
[10] J. Mai, A. Casties, and W. Von Niessen, Chem. Phys. Lett. **196**, 358 (1992).
[11] A. Yu. Tretyakov and H. Takayasu, Phys. Rev. A **44**, 8388 (1991).
[12] S. B. Lee, Physica A **387**, 1567 (2008).
[13] E. V. Albano, Surf. Sci. **235**, 351 (1990); Phys. Rev. B **42**, 10818 (1990).
[14] A. Casties, J. Mai, and W. von Niessen, J. Chem. Phys. **99**, 3082 (1993).
[15] D. Sornette, Phys. Rep. **297**, 239 (1998).
[16] M. A. Bab, G. Fabricius, and E. V. Albano, EPL **81**, 10003 (2008).
[17] I. Jensen, J. Phys. A **32**, 5233 (1999).
[18] C. A. Voigt and R. M. Ziff, Phys. Rev. E **56**, R6241 (1997).
[19] P. Grassberger, J. Phys. A **22**, 3673 (1989).
[20] M. A. Bab, G. Fabricius, and E. V. Albano, Phys. Rev. E **74**, 041123 (2006).
[21] M. A. Bab and E. V. Albano, Eur. Phys. J. B **63**, 521 (2008).
[22] M. A. Bab, G. Fabricius, and E. V. Albano, J. Chem. Phys. **128**, 044911 (2008).
[23] M. A. Bab and E. V. Albano, J. Phys. A **41**, 045001 (2008).
[24] A. L. Maltz, G. Fabricius, M. A. Bab, and E. V. Albano, J. Phys. A **41**, 495004 (2008).
[25] P. J. Grabner and W. Woess, Stochastic Proc. Appl. **69**, 127 (1997).
[26] E. Teufl, Combinatorics, Probab. Comput. **12**, 203 (2003).
[27] B. Krön and E. Teufl, Trans. Am. Math. Soc. **356**, 393 (2004).
[28] M. A. Muñoz, G. Grinstein, and Yuhai Tu, Phys. Rev. E **56**, 5101 (1997).